PCCP

Accepted Manuscript

ROYAL SOCIETY OF CHEMISTRY

www.rsc.org/pccp

Di- and tri-oxalkyl derivatives of a boron dipyrromethene (BODIPY) rotor dye in lipid bilayers

Marie Olšinová[†#], Piotr Jurkiewicz[†#], Michal Pozník[‡], Radek Šachl[†], Tereza Prausová[‡], Martin Hof[†], Václav Kozmík[‡], Filip Teplý[§], Jiří Svoboda[‡], and Marek Cebecauer[†*]

[†]Department. Biophysical Chemistry, J. Heyrovsky Institute of Physical Chemistry, Academy of Sciences of the Czech Republic, v. v. i., Dolejškova 3, 18223 Prague, Czech Republic; [‡]Department of Organic Chemistry, Institute of Chemical Technology, Prague, Czech Republic; [§]Institute of Organic Chemistry and Biochemistry, Academy of Sciences of the Czech Republic, v. v. i., Flemingovo nám. 2, 18223 Prague, Czech Republic

[#] These authors contributed equally.

* Corresponding Author: Marek Cebecauer, J. Heyrovsky Institute of Physical Chemistry of the AS CR, Dolejskova 3, 18223 Prague , Czech republic; Tel.: +420-26605 3733; Email: marek.cebecauer@jh-inst.cas.cz

KEYWORDS: lipid membrane, fluorescent probe, molecular rotor, lipid packing, probe orientation, fluorescence lifetime microscopy, anisotropy.

ABSTRACT

The environment-sensitive fluorescent probes provide excellent tool for studying membranes in their native state. We have modified BODIPY-based fluorescent molecular rotor by increasing the number of alkyl moieties from one to two or three to achieve a more defined and deeper positioning of the probe in membranes. Detailed characterisation of fluorescence properties and localisation/orientation of probes was performed using a variety of fluorescence techniques and model membranes composed of different lipids. As expected, additional alkyls attached to the fluorophore moiety led to a deeper and more defined localisation of the probe in the lipid bilayer. The results strongly indicate that fluorescence properties of such probes are influenced not only by lipid packing but also by the orientation of the probe in membranes. The orientation of herein studied rotors was significantly altered by changes in lipid composition of membranes. Our observations demonstrate the limits of BODIPY-based molecular rotors as environmental sensors in cellular membranes with complex lipid composition. Herein presented results also underline the importance of detailed characterisation of fluorescent membrane dyes and provide a guide for future testing.

Introduction

Physical properties of membranes regulate processes as diverse as cell division, signalling, or infection by viruses and other microbes. [1-4] In addition, membrane properties may influence the effectiveness of drug targeting. [5,6] It is therefore important for biologists, clinicians and drug designers to characterise membranes in their native environment.

Fluorescence microscopy provides the best tool for studying living cells and organisms. Microenvironment-sensitive fluorescent probes are used to investigate properties of cellular compartments such as the cytosol, mitochondria or membranes. [6] Transmembrane potential, surface charge, morphology and lipid packing are the most frequently tested properties of cellular membranes. Protein domain-based probes function as sensors of the changes of the surface charge and curvature in living cells. [7-9] Such probes associate peripherally with the membrane of defined properties. On the contrary, small fluorescent probes sensing the membrane potential, morphology and lipid packing are localised in close proximity to or within the hydrophobic core of the lipid bilayer. Morphology-sensing probes report on their exact orientation within the membrane using polarisation-dependent fluorescence measurements. [10,11] Probes reporting on membrane potential belong to electro- and solvatochromic dyes. [12] Solvatochromic dyes are also used for the characterisation of membrane lipid packing. [6] Solvatochromic fluorescent probes change their emission spectra due to the relaxation in the presence of polar molecules (e.g. water) in their vicinity. In lipid bilayers this relaxation reports on local polarity (hydration) and mobility of the hydrated lipid moieties. Such mobility is sometimes interpreted in terms of membrane viscosity.

It is important to note here that viscosity (as well as “microviscosity” or fluidity) of membranes differs from the viscosity of bulk solutions. Viscosity is by definition a macroscopic parameter. Its use in nanoscale is an approximation that provides an intuition, but might be also misleading. [13] This issue is discussed in more details in Conclusions. Throughout this paper we use the term viscosity to talk about lipid packing and mobility in membranes and in particular how they affect rotation of membrane embedded fluorescent probes.

One of the directions in the design of fluorescent viscosity probes is focused on the fluorophore rotation in membranes. For example, a capacity of fluorescence anisotropy to report on the rotation of rigid linear fluorophores embedded in the membranes was explored. Fluorescence anisotropy of DPH embedded in the hydrophobic core of the bilayer can give an estimate of membrane fluidity [14] and the lipid acyl chain order. [15] The disadvantage of DPH is its excitation by the physiologically unfriendly UV light. It is well established that the fluorescence of molecular rotors depends on a relative viscosity of the surrounding environment in model and biological systems. [16,17] The viscosity of the surrounding molecules modulates the extent of intra-molecular twisting of the chromophore which directly influences experimentally well accessible parameters such as fluorescence quantum yield or lifetime. Originally, julolidine-based molecular rotors were developed for viscosity measurements in cells. [18] These probes are excited in live cell-incompatible spectral region 300-450 nm limiting their use to non-cellular systems. Moreover, it was reported that these probes respond more to the porosity of a material (free volume effect) and less to its viscosity. [19] More recently, boron dipyrromethen (BODIPY)-based molecular rotors were developed for probing viscosity in membranes. [20-22] These probes composed of the BODIPY dipyrromethene framework and a phenyl group emit fluorescence only from the metastable twisted conformation, but not from the planar one (depicted in Figure 1). Indeed significant changes in fluorescence lifetime were observed in solutions of glycerol with different viscosities. However, fluorescence lifetime images of BODIPY-based molecular rotors [21] do not provide clear information when applied to cellular membranes. Recent fluorescence lifetime measurements presented by Kuimova and colleagues [22] show biexponential decays suggesting heterogeneous

localisation/orientation of this probe in model membranes with different lipid phases. Based on their findings, we have predicted this is caused by poor incorporation of mono-acylated BODIPY-based rotor in lipid bilayers.

Undefined location and orientation of probes in general hampers their use for sensing changes in membrane properties. Indeed, for higher sensitivity, fluorescent membrane probes need to be localised within the hydrophobic part formed largely by acyl chains of phospholipids or in the lower part of lipid headgroup (close to the carbonyl moiety; refs. 23-25). No information on the localisation and orientation of BODIPY-based fluorescent molecular rotors is available.

The aim of this work was to improve the membrane localisation of BODIPY-based molecular rotor by increasing the number of alkyl chains attached to the fluorophore moiety. All generated probes were tested for their capacity to function as molecular rotors and to distinguish between model membranes in different lipid phases. In addition, we thoroughly determined localisation and orientation of newly synthesised fluorescent probes in lipid bilayers and compared those to the previously used mono-alkyl BODIPY molecular rotor derivative. [21]

Experimental Section

Chemicals. All chemicals and organic solvents were purchased from Sigma-Aldrich and Merck, or otherwise stated. 1,2-dimyristoyl-*sn*-glycero-3-phosphocholine (DMPC), 1-palmitoyl-2-oleoyl-*sn*-glycero-3-phosphocholine (POPC), 1,2-dioleoyl-*sn*-glycero-3-phosphocholine (DOPC), 1,2-dipalmitoyl-*sn*-glycero-3-phosphocholine (DPPC), 1,2-dipalmitoyl-sn-glycero-3-phosphoethanolamine-*N*-(cap biotinyl) (biotinylated-DPPE), 1-palmitoyl-2-stearoyl-(16-doxyl)-*sn*-glycero-3-phosphocholine (16-Doxyl), 1-palmitoyl-2-stearoyl-*sn*-glycero-3-phosphocholine (PSPC) and cholesterol were purchased from Avanti Polar Lipids, Inc. (Alabaster, AL, USA), streptavidin from IBA (Goettingen, Germany), acrylamide from (Fluka, Switzerland), $DiIC_{18}$ (5)-DS (DiD) from Invitrogen (Carlsbad, CA).

Synthesis of di- and tri-oxalkyl derivatives of boron dipyrromethene (BODIPY) molecular rotor dyes. Synthesis of the new BODIPY dyes **2a**, **2b**, **3a**, **3b** (Figure 1) was performed by the condensation of pyrrole and 2-methylpyrrole with 3,5-didodecyloxybenzaldehyde and 3,4,5-tridodecyloxybenzaldehyde, respectively, by the reported methodology. [26] Details of the synthesis are in the Supplementary material. Compound **1** was synthesised as described before. [21]

Characterisation of fluorescent properties of the probes. Since the studied probes are practically insoluble in water, sparingly soluble in ethanol and DMSO, and only weakly soluble in methanol, their spectral properties were studied in methanol:chloroform 1:1, v:v. The measurements were performed in standard 1 cm quartz cuvettes (Hellma GmbH, Germany) at room temperature, except the temperature scans of the dyes embedded in DMPC LUVs, for which the temperature was maintained at 10, 15, 20, 25, 30, and 40°C within ± 0.5°C using a water-circulating bath. Absorbance was measured using Helios Gamma UV-vis spectrophotometer (Unicam Ltd., UK). Emission and excitation spectra were collected using fluorolog-3 FL3–11 spectrofluorimeter (Jobin Yvon Inc., Edison, NJ, USA) equipped with a xenon-arc lamp. The spectra where corrected for the sensitivity of the detectors. Absorbance of the samples was kept below 0.1 to minimize the inner filter effect. Fluorescence quantum yields were calculated according to: $\Phi = \Phi_R \times F/F_R \times A_R/A \times n^2/n_R^2$, where Φ – quantum yield, A – absorbance, F – fluorescence intensity, n – refractive index, R subscript denotes values for the reference solution of Rhodamin 6G in ethanol: Φ_R=0.94 [27], n_R (ethanol) = 1.36, n (methanol:chloroform, 1:1, v:v) = 1.39.

Cuvette-based fluorescence lifetime measurements of the probes embedded in large unilamellar vesicles (LUVs) were performed using a 5000U Single Photon Counting setup using cooled Hamamatsu R3809U-50 microchannel plate photomultiplier. All decays were fitted with multi-exponential function using the iterative reconvolution procedure (IBH DAS6 software). Fluorescent probes were excited with pulsed diode lasers 470 nm LDH-P-C-470 and 506 nm LDH-D-C-510 (PicoQuant, Germany). Additionally, the emission long pass 500 nm cut-off filter was used to eliminate the scattered light.

Preparation of lipid vesicles. Multilamellar vesicles (MLVs) were prepared as follows: Chloroform solutions of appropriate lipids were mixed in a glass tube with a probe solution to obtain the final probe to lipid ratio of 1 mol%. Organic solvents were evaporated under stream of nitrogen while continuously heated and then under vacuum for at least 1 hour. The dry lipid film was suspended in 10 mM Hepes (pH=7.4, 150 mM NaCl) buffer and vortexed for 4 minutes at ~40°C. To obtain LUVs, the MLVs were extruded through polycarbonate membrane with effective pore diameter of 100 nm (Avestin, Ottava, Canada), 50 passages, at ~40°C.

Small unilamellar vesicles (SUVs) were prepared in the same way except the extrusion was substituted with sonication for 5 min using tip sonicator (Sonopuls HD 2070, Bandelin electronic GmbH, Germany) at 25% power, while cooled in a water bath at room temperature. Oxygen was removed from the sample before the sonication by a gentle stream of argon. SUV samples were not centrifuged to keep the lipid content unchanged.

For preparation of GUVs: DOPC lipid was used for liquid-disordered phase (Ld), DPPC (66 mol%) and cholesterol (30 mol%) for liquid-ordered phase (Lo), DPPC for solid phase (So) and DOPC (33 mol%), DPPC (33 mol%) and cholesterol (30 mol%) for phase-separated (Ld+Lo) vesicles. All lipid mixtures contained 4 mol% of biotinylated-DPPE for the attachment of vesicles to the BSA-biotin/streptavidin coated glass coverslips to reduce their mobility. GUVs were prepared by electroformation according to Stöckl and co-workers. [28] Briefly, 100 nmol of lipids in chloroform (total volume 100 µl) containing BODIPY rotor dye (rotor:lipid = 1:1000) were spread on two preheated titanium slides. Slides were kept for 1 hour in vacuum to evaporate any residual solvent. The slides were than stuck together by melting parafilm. Formed chamber was filled with 100 mM sucrose in water and heated to 50°C followed by applying the sinusoidal altering voltage (10 Hz): starting at 150 mV (peak-to-peak amplitude) and gradually increasing with step of 50 mV every 2.5 min up to 1.1 V, this voltage was held for another 90 minutes. At the end, the frequency of 4 Hz and the voltage of 1.3 V were applied for 30 minutes for detachment of vesicles. GUVs were transferred into LabTek 8-well chamber slide (ThermoScientific; Waltham, USA) coated with BSA-biotin/streptavidin. Landing of GUVs to the optical surface was enabled by changing the buffer in the chamber for cca 61 mM glucose, 10 mM HEPES and 10 mM NaCl which has the same osmolality as sucrose buffer (103 mOsm). Within one hour, GUVs were firmly attached to the coated glass surface and ready for imaging.

Fluorescence lifetime imaging (FLIM) and phasor plot analysis. Measurements were performed on a MicroTime 200 inverted confocal microscope (PicoQuant, Berlin, Germany) with a water immersion objective (1.2 NA, 60×) (Olympus, Hamburg, Germany) and main dichroic mirror 509 (Chroma, Rockingham, VT). Pulsed diode laser (506 nm, LDH-D-C-510, PicoQuant) with 20 MHz repetition rate was employed for excitation and the signal was detected by single photon avalanche diodes using 530/10 band pass filter (Chroma). Laser intensity was kept below 300 nW (at sample location). Each GUV was scanned in the cross section; 512 x 512 pixels (0.6 ms/pixel). Acquired images containing fluorescence lifetime data were analysed by standard decay fitting and by phasor plot analysis which enables direct presentation of fluorescence lifetime image data without the requirement of decay fitting. [29] Phasor plot analysis: by Fourier transformation of decay from every image pixel, we obtain coordinates that assign pixel decay to phasor plot. Accumulation of points in phasor plot creates “hot spot(s)” that characterise the lifetime distribution in the

image. A fluorescence probe with monoexponential decay generates spot that is located at the universal circle, those with multiexponential decay inside the universal circle (Figure S1a). Phasor plot analysis enables colour-coded localisation of image pixels that contribute to the selected point(s)/area(s) of the phasor plot (e.g. Figure S2c).

Anisotropy measurements. Fluorescence anisotropy measurements were performed on MicroTime 200 inverted confocal microscope as described for FLIM. Pulsed diode laser (470 nm, LDH-P-C-470, PicoQuant) with 20 MHz repetition rate was used. The signal was detected by single photon avalanche diodes (SPAD) using 515/50 band pass filter (Chroma). For anisotropy measurements, the linear polariser (Thorlabs) was inserted into the excitation pathway to modulate polarisation of the light (horizontal alignment was used exclusively). Polarisation beam splitter (Ealing, UK) was placed in front of SPAD detectors to separate vertically and horizontally polarised emitted light. Laser intensity was kept below 300 nW (at sample location). Each GUV was scanned in the *XY* plane cross section; an image of 256 x 256 pixels (1.2 ms/pixel) was acquired. Images were analysed using Matlab procedure. Anisotropy was calculated for every pixel as: $R = (I_{\parallel} - G \times I_{\perp}) / (I_{\parallel} + 2 \times G \times I_{\perp})$, where $I_{\parallel}$ and $I_{\perp}$ are the intensities of the horizontally and vertically polarised fluorescence, respectively. G factor was obtained from the measurement of free diffusing carboxy-fluorescein in NaOH, the flurescence decays of which were analysed using a tail matching method implemented in FluoFit v.4.5 (PicoQuant, Berlin, Germany). Additional details of the analysis and the code of the Matlab procedure are provided in the Supplementary information.

Acrylamide quenching. Fluorescent probes (**1**, **2b** and **3b**) embedded in POPC LUVs were quenched using acrylamide, which was titrated to the cuvette containing the liposomal suspension, while the fluorescence intensity was continuously measured. Both the samples and the acrylamide solution were kept at room temperature. Quenching data were analysed using the Stern-Volmer equation: $F_0/F = 1 + K_D \times [Q]$, where F_0 and F are the fluorescence intensities in the absence and the presence of the quencher, respectively, K_D is the Stern-Volmer quenching constant, and [*Q*] is the concentration of the quencher in the sample.

16-doxyl quenching. For the spin-label quenching MLVs composed of 84 mol% of DPPC, 1 mol% of a fluorescent probe, and 15 mol% of either 16-Doxyl or PSPC were used. Fluorescence emission spectra of MLV suspensions were measured at 60°C (Ld phase) and integrated to obtain fluorescence intensities in the absence and presence of the quencher: F_0 and F, respectively.

Localisation of fluorescent probes by Förster resonance energy transfer (FRET). In a lipid bilayer the excitation energy can be transferred either to an acceptor molecule localised in the same leaflet, or to one in the opposite leaflet. In the former process, the survival probability $G_{\text{intra}}(t)$, i.e. the probability that the excited probe is still in the excited state after the time t, is referred to as intra-FRET and can be expressed as [30]

$$\ln G_{\text{intra}}(t) = -C_2 \Gamma\left(\frac{2}{3}\right)\left(\frac{t}{\tau}\right)^{1/3}. \qquad (1)$$

Here, C_2 is a so-called reduced surface concentration of acceptors and equals the number of acceptor molecules found in the area of a circle with the Förster radius R_0 surrounding a donor, Γ is a so-called lambda function and τ is the lifetime of the donor.

When the energy is transferred across the bilayer the process is referred to as inter-FRET and $G_{\text{inter}}(t)$ is given by [30]

$$\ln G_{\text{inter}}(t) = -\frac{C_2}{3}\left(\frac{d}{R_0}\right)^2\left(\frac{2\nu}{3}\right)^{1/3}\int_0^{\langle\kappa^2\rangle\nu}(1-e^{-s})s^{-4/3}ds, \quad (2)$$

where d is the plane to plane distance of donors from the acceptors (intra- and inter-leaflet distances d_A and d_B can be considered; Figure 3), and $s = \frac{3}{2}\left(\frac{R_0}{d}\right)^6 \cos^6\theta_r \langle\kappa^2\rangle \frac{t}{\tau} = \nu\langle\kappa^2\rangle \cos^6\theta_r$. In the last equation ϑ_r and $\langle\kappa^2\rangle$ denote the angle between the bilayer normal and the vector connecting the donor and the acceptor and the mean square average of the angular part of the dipole-dipole interaction.

The fluorescence decay of a donor in the presence of acceptors can be obtained by multiplication of the total survival probability $G_{\text{tot}}(t) = \prod_j G_{j,\text{inter/intra}}(t)$ with the fluorescence decay of the donor in the absence of acceptors

$$F(t) = G_{\text{tot}}(t) F_D(t). \quad (3)$$

The compounds are localised by fitting the experimental decay curves to the above equations. Position of the compounds is determined by the plane to plane distance *d* (Figure 3), which is one of the optimised parameters. Experimental TRF decays were obtained on LUVs (DOPC) using experimental setup as for the characterisation of fluorescent properties of the probes but adding polarisation filter. Donor was represented by compounds **1, 2b** and **3b**, respectively, acceptor by DiD (see Supplementary Information for DiD membrane localisation measurements). The donor/acceptor to lipid ratios were 1:1000/1:200, respectively.

Results and Discussion

Localisation of the probes. Well-defined positioning of fluorescent dyes probes is essential for their capacity to report on changes in the environment such as biological membranes. Variation in positioning of BODIPY-based membrane molecular rotor was observed [22] in membranes with higher lipid ordering and in the presence of cholesterol, an essential component of biological membranes. This influences fluorescence properties of such probe and limits its use in membranes with higher lipid ordering and sterol content such as the plasma membrane of eukaryotes. The BODIPY-based rotor used in the study [22] was designed with single alkyl (C_{12}) moiety. Phospholipids present in biological membranes contain prevalently two acyl chains. Therefore, we designed and synthesized di- and tri-alkylated variants of the BODIPY-based rotor to improve its positioning in lipid membranes. Synthesis of the compounds **2a**, **2b**, **3a** and **3b** (Figure 1) was performed by the condensation of pyrrole and 2-methylpyrrole with 3,5-didodecyloxybenzaldehyde and

3,4,5-tridodecyloxybenzaldehyde, respectively, by the reported methodology (ref. 26, see also Supplementary Information). Compound **1** was synthesised as described before. [21] UV/Vis measurements revealed expected spectra with excitation maxima at 501 and 500 nm and emission maxima at 518 and 517 nm for compounds **2a** and **3a**, respectively (Figure 2a). 3,5-methylated forms of the rotors (compounds **2b** and **3b**) provided higher fluorescence intensities due to increased extinction coefficient and quantum yield in methanol:chloroform mixture, 1:1 (Table 1). The fluorescence properties of the newly synthesized compounds **2b** and **3b** were comparable to the previously reported BODIPY-based molecular rotor (compound **1**; Table 1; ref. 21). In order to test the function of new compounds as viscosity sensors in membranes, their fluorescent molecular rotor properties were characterised in lipid vesicles composed of DMPC. By changing temperature from 10 to 40°C we induced changes of viscosity in membranes and, therefore, the ability of fluorescent dye to rotate. Changes in fluorescence lifetimes of compounds **2a**, **2b**, **3a** and **3b** correlate with viscosity in membranes, therefore, these probes can be considered as fluorescent molecular rotors (Figure 2b/Table 1). A rapid change in fluorescence lifetime indicates that new compounds have propensity to sense phase transition of DMPC (23.6 ± 1.5)°C . [31] Such property was not observed for compound **1** under tested conditions. Compounds **2b** and **3b** were selected for further analyses due to their superior fluorescence properties compared to compound **2a** and **3a**.

Di- and trialkylation of BODIPY molecular rotor was proposed to improve positioning of the dyes with respect to the hydrophobic core of lipid bilayer. Therefore, we first investigated the positioning of compounds **1**, **2b** and **3b** in model membranes. Fluorescence of the probes **1**, **2b** and **3b** embedded in POPC vesicles was quenched by water-soluble quencher – acrylamide, and by free radical quencher – 16-Doxyl located in the centre of the bilayer. Acrylamide does not penetrate into the lipid bilayer, thus

the changes in the obtained quenching constants (Table 1) measured for POPC LUVs reflect the changes in fluorophores availability (exposure) to the aqueous phase, thus the depth of their location within the bilayer. All the Stern-Volmer constants are very low. This low efficiency of acrylamide quenching is typical for BODIPY-based dyes (R.S., unpublished data). Nevertheless, the quenching constants for compounds **2b** and **3b** are two to three times lower than the one measured for compound **1**, which suggests their deeper location in the membrane. For the quenching with 16-Doxyl DPPC MLVs with 15 mol% of either 16-Doxyl, or DSPC (control), were measured at 60°C. The resulting F_0/F ratios are given in Table 1. The quenching was observed for all three compounds, and its efficiency increased in the row: **1** << **2b** < **3b**. The efficiency of the quenching is inversely proportional to the distance between the fluorophore and the bilayer centre, where the spin label is located. Thus, the depth of the location of the compounds increases in the same order.

The quenching results support our prediction that by increasing the number of the alkyl chains attached to the probe will improve the membrane localisation of the fluorescence molecular rotor: the newly synthesized compounds **2b** and **3b** are located deeper in the bilayer compared to the compound **1**.

Further information on the localisation of fluorescence probes can be obtained by a detailed analysis of the time-resolved fluorescence (TRF) decays of the dyes. The experiment is based on Förster resonance energy transfer and has been designed in the following way: the compounds **1**, **2b** and **3b**, which served as donors of the excitation energy, were incorporated into the DOPC bilayer together with acceptor molecules represented by a lipid marker DiD. While the position of donors is unknown, the chromophore of DiD is well localised at the lipid-water interface. The rate of energy transfer, and by that the shape of TRF decays, depends on the overall surface concentration of DiD acceptors but also on the plane to plane distance of the donors from the acceptors (cf. eq. 1-3). Since position of DiD molecules is a priori known, the position of the donors with respect to the acceptors can be determined (Figure 3). The plane to plane distance d_B of 36 Å for compound 1 or 33 Å for compounds **2b** and **3b**, respectively, was obtained by fitting of TRF decays to the equations (see Material and Methods). Since the goodness of the fit was not influenced by the shorter plane to plane distance d_A in the range of physically relevant distances, d_A could not be determined from the TRF decays. To conclude this section, both the FRET and quenching data indicate that compounds with more than one alkyl chain reside deeper in the lipid bilayer than those with one alkyl chain only.

Sensitivity of the fluorescence lifetime to the bilayer viscosity. The new compounds **2b** and **3b** exhibit fluorescent properties similar to those of the compound **1** (original BODIPY-based rotor) but are localised deeper within lipid bilayers. We tested their propensity to report on membrane's lipid phase state and, thus, viscosity. Dependence of fluorescence lifetime on lipid phase was investigated. FLIM measurements of compounds **1**, **2b** and **3b** were performed on GUVs composed of DOPC (Ld phase), DPPC:cholesterol (2.2:1; Lo phase), and DPPC (So phase). TRF decays were processed by standard mono-/bi-exponential fitting and using fit-free phasor plot analysis.

In contrast to the original BODIPY-based molecular rotor (compound **1**), compounds **2b** and **3b** exhibited only weak biexponential fluorescence decay irrespective of the studied lipid phase (Figures 4 and S1b). This indicates we have reached a more defined positioning of compounds **2b** and **3b** in lipid membranes with varying viscosity by increasing the number of alkyl chains attached to the rotor moiety. Surprisingly, the improved membrane positioning was accompanied by reduced capacity of compounds **2b** and **3b** to distinguish fine changes in lipid packing in membranes with different composition. No significant difference in lifetimes measured in Ld (DOPC) and Lo (DPPC:cholesterol; 2.2:1) phases was detected for compounds **2b** and **3b** (Table 2). On the contrary, well distinguishable lifetimes were measured for GUVs with liquid (Ld or Lo) and gel (So) phases (Table 2). By observing vesicles with different lipid composition (Ld and So phase) in the same field of view, fluorescence lifetime measurements for

compounds **2b** and **3b** provided sufficient information to determine liquid or solid character of lipids in the particular vesicles (Figure S2). For compound **1**, we measured different mean fluorescence lifetimes for vesicles in Ld (1.8 ± 0.1 ns), Lo (2.9 ± 0.1 ns) and So (4.5 ± 0.2 ns) phases indicating a better capacity of this probe to function as environmental sensor in membranes compared to compounds **2b** and **3b**. In agreement with previous report [22], we observed bi-exponential decay of fluorescence lifetime for compound **1** in membranes with Lo and So phases which indicates heterogeneous positioning of the probe with respect to the membrane. Such undefined positioning limits the use of compound **1** for measurements in membranes with higher lipid ordering (e.g. Golgi apparatus, exo-, endosomes and the plasma membrane of mammalian cells). Of note, all tested compounds when investigated in vesicles with separated phases (coexisting Ld and Lo phases; DOPC:DPPC:cholesterol 1:1:0.9) extensively located to the Ld phase similar to a majority of available membrane probes. [32] Such observation again limits the use of BODIPY-based molecules rotors as environment-sensitive probe in complex membranes such as cellular membranes.

Reorientation of the probes. In FLIM experiments, we have observed spatially uneven fluorescence intensity distribution in GUV cross-sections for compounds **1**, **2b** and **3b** in all tested lipid compositions (an example in Figure S3). Such observation implies that the fluorescence of the dye depends on its orientation with respect to the polarisation of the excitation light; i.e. indicates a preferential orientation of the chromophore in membranes. Surprisingly, such a fluorescence intensity distribution for compound **3b** in GUV is different for the Ld and So phases (Figure 5). Since this is likely to be an effect of the pre-selection of oriented fluorophores upon excitation we decided to investigate this effect using fluorescence confocal polarisation microscopy. Anisotropy *XY* cross-section images of the GUVs composed of DOPC (Ld phase) and DPPC (So phase) were calculated from the images measured separately for the emission light polarised parallel and perpendicular to the excitation light (polarised horizontally). Defining fluorescence anisotropy under the setup of a confocal microscope is a difficult task. This is due to complex optics and the use of high numerical aperture objectives, which changes the light polarisation in a nontrivial way. [33] Moreover, in the case of an oriented sample the total intensity is no longer given by: $I_{\parallel} + 2\times G\times I_{\perp}$ (ref. 34), which can be overcome by studying linear dichroism instead of anisotropy. [35] Nevertheless, herein we use the standard anisotropy equation. This gives only a crude approximation of the real anisotropy, but serves well the purpose of investigating the fluorophore orientation within the lipid bilayer. The examples of anisotropy images obtained for compounds **1**, **2b** and **3b** are shown in Figure 5. Non-uniform anisotropy was detected for all tested compounds in both, Ld and So phases, i.e. anisotropy depends on the orientation of the bilayer in respect to the polarisation of the excitation light (green arrow in Figure 5). These changes in anisotropy do not reflect changes in the fluorophore reorientation kinetics which is uniform throughout the GUV. They rather result from the changes of the fluorophore orientation with respect to the polarisation of the excitation light leading to the excitation pre-selection. This confirms the results observed during FLIM experiments. The anisotropy images were further analysed and the angular dependence of the anisotropy along the GUV cross-section was calculated (Figure 5 c, g, k). The sinusoidal dependence of the anisotropy in Ld GUVs (DOPC, black curves) is very similar for all three probes. Its amplitude is smaller for compound **2b** compared to the two other probes, suggesting a non-uniform orientation of this compound in the lipid bilayer. The anisotropy maxima (observed at ± 90°) indicate the average orientation of probes with their transition dipole moment vector along the vector of excitation polarisation, while the anisotropy minima at 0° and 180° indicate perpendicular orientation of the two vectors. Assuming the uniform distribution and orientation of probes within the GUV membrane, the discussed results show that fluorophore is orientated with its dipole moment perpendicular to the membrane normal (parallel to the surface), as schematically depicted for Ld phase in the right panel of Figure 5 (black arrows). In other words the compounds are oriented in the Ld membrane just as they are depicted in the scheme in Figure 1. Different results were achieved using vesicles with So phase (DPPC). Distinct anisotropy plot was determined for each of tested probes. The anisotropy plot for compound **1** is similar for Ld

and So phases (Figure 5c). The amplitude of the anisotropy is increased in the So phase compared to the Ld phase, manifesting a more rigid environment, but the orientation of the probe is the same. For the two other probes a re-orientation was observed. There is an evident 90° shift of the anisotropy profile for compound **3b** upon transition from Ld to So phase, which we interpret as a re-orientation of the fluorophores within the membrane, as schematically depicted in the right panel of Figure 5 (blue arrows). A more complex picture emerges for compound **2b** in the So phase vesicles, i.e. the maxima are present at ± 90° and at 0° and 180°. This suggests the existence of two populations (orientations) of the compound **2b** in So phase: one oriented perpendicular and one parallel to the membrane normal (Figure 5h). Our fluorescence lifetime and anisotropy data indicate multifaceted effect of membrane lipid composition and viscosity on the fluorescence properties and positioning/orientation of herein studied BODIPY-based molecular rotor (compounds **1**-**3**) dyes thereby limiting the usage of these probes in complex membranes.

Conclusions

It is now decades since the design and synthesis of the first environment-sensitive fluorescent probes which accelerated membrane research and enabled studies in cells. [36] Here we tried to improve the localisation of BODIPY-based molecular rotor originally designed for sensing viscosity in membranes. [21] The original probe suffers from unclear localisation of the probe in membranes with higher lipid packing. [22] We have achieved significant improvement in the localisation of the dye deeper in the lipid bilayers by increasing the number of C12 alkyl chains linked to the fluorophore moiety from one to two or three - compounds **2b** and **3b**. Our probes exhibit predicted fluorescence properties of the molecular rotor (Table 1). Detailed characterisation of these probes using a variety of fluorescence techniques uncovered a complex positioning/orientation of all tested probes within membranes with different lipid composition. Such results indicate that BODIPY-based molecular rotors may be employed for measurements of lipid packing in membranes composed of simple lipid mixtures in liquid disordered phase but not in more complex membranes such as cellular membranes or cell-derived vesicles. [37-38]

As already mentioned in the introductory chapter, viscosity is a poorly-defined parameter for lipid membranes. The Saffman-Delbrück (SD) [39] and Hughes–Pailthorpe–White (HPW) [40] models accurately describe lateral diffusion of molecules in lipid bilayers [41] but they describe the membrane as a two-dimensional structure-less fluid and diffusing particle as a solid cylinder spanning the membrane. This holds remarkably well for lateral diffusion of a number of proteins or membrane domains. [41-42] But, for molecular rotors in lipid bilayers measured fluorescence is influenced by at least two factors: i) The viscosity in the hydrophobic core and in the headgroup region of the bilayer differs which is in conflict with SD and HPW models predicting uniform viscosity along the membrane normal. Molecular rotors can interact locally with both parts of the membrane. ii) The measured fluorescence can be prone to a specific lipid composition, or probe re-location/re-orientation, as we have shown here. And finally, it was shown in isotropic media that molecular rotors are susceptible to free volume effects (refs. 13, 19). This effect has not been tested in membranes yet.

Although it is unfortunate that membrane molecular rheology still lacks a properly defined parameter that could be intuitively compared to the viscosity of the bulk solution, molecular rotors are still useful experimental tools. When carefully used they can provide valuable information on local lipid packing and mobility. Further development of such probes focused on stability of their membrane location should further increase their applicability. One option here may be to better mimic natural lipids.

ASSOCIATED CONTENT

Supplementary material contains detailed Experimental part (synthesis of compounds), Supplementary Figures S1-S4 and MATLAB script for the analysis of anisotropy data from confocal microscopy fluorescence lifetime images.

ACKNOWLEDGMENT

We would like to thank company PicoQuant for kind lending of the pulsed 509 nm laser. We would also like to thank Peter Kapusta and Martin Stefl for their technical help and Dylan Owen for critical reading of the manuscript.
We are pleased to acknowledge funding by Czech Science Foundation (P305/11/0459). M.C. would like to thank for Purkyne Fellowship and M.H. Praemium Academie of the Academy of Sciences of the Czech Republic.

ABBREVIATIONS

Biotinylated-DPPE, 1,2-dipalmitoyl-*sn*-glycero-3-phosphoethanolamine-*N*-(cap biotinyl); BODIPY, boron-dipyrromethen; BSA-biotin, bovine serum albumin, biotin labelled; DiD, 1,1'-dioctadecyl-3,3,3',3'-Tetramethylindodicarbocyanine Perchlorate; DMPC, 1,2-dimyristoyl-*sn*-glycero-3-phosphocholine; DOPC, 1,2-dioleoyl-*sn*-glycero-3-phosphocholine; DPPC, 1,2-dipalmitoyl-*sn*-glycero-3-phosphocholine; FLIM, fluorescence lifetime imaging microscopy; FRET, Förster resonance energy transfer; GUVs, giant unilamellar vesicles
Ld, liquid disordered lipid phase; Lo, liquid ordered lipid phase; LUVs, large unilamellar vesicles; MLVs, multilamellar vesicles; POPC, 1-palmitoyl-2-oleoyl-sn-glycero-3-phosphocholine; PSPC, 1-palmitoyl-2-stearoyl-*sn*-glycero-3-phosphocholine; So, solid lipid phase; SUVs, small unilamellar vesicles; TRF decays, time-resolved fluorescence decays; 16-doxyl, 1-palmitoyl-2-stearoyl-(16-doxyl)-*sn*-glycero-3-phosphocholine.

AUTHOR CONTRIBUTIONS

M.O. performed fluorescence measurements and contributed to the writing of manuscript, P.J. designed and performed fluorescence experiments and contributed to the writing of manuscript, M.P. performed synthesis of compounds, R.S. designed experiments and contributed to the writing of manuscript, T.P. performed synthesis of compounds, M.H. contributed to the design of experiments, V.K. helped with the synthesis of compounds, F.T. design of synthesis, J.S. design of synthesis and writing of manuscript, M.C. design of experiments and writing of manuscript.

REFERENCES

1. D. Owen, K. Gaus, A. Magee and M. Cebecauer, Immunology, 2010, 131, 1-8.
2. M. Edidin, Nat Rev Mol Cell Biol, 2003, 4, 414-418.
3. S. R. Shaikh and M. A. Edidin, Chem Phys Lipids, 2006, 144, 1-3.
4. G. van Meer, D. R. Voelker and G. W. Feigenson, Nat Rev Mol Cell Biol, 2008, 9, 112-124.
5. N. E. Caceres, M. Aerts, B. Marquez, M. P. Mingeot-Leclercq, P. M. Tulkens, B. Devreese and F. Van Bambeke, PLoS One, 2013, 8, e58285.
6. Y. Mely and G. Duportail, Fluorescent Methods to Study Biological Membranes, Springer Verlag, Heidelberg, 2013.
7. B. Antonny, Annu Rev Biochem, 2011, 80, 101-123.
8. G. Drin, V. Morello, J. F. Casella, P. Gounon and B. Antonny, Science, 2008, 320, 670-673.
9. T. Yeung, G. E. Gilbert, J. Shi, J. Silvius, A. Kapus and S. Grinstein, Science, 2008, 319, 210-213.
10. A. P. Demchenko, Y. Mely, G. Duportail and A. S. Klymchenko, Biophys J, 2009, 96, 3461-3470.
11. S. E. Sund, J. A. Swanson and D. Axelrod, Biophys J, 1999, 77, 2266-2283.
12. A. S. Klymchenko and A. P. Demchenko, Methods Enzymol, 2008, 450, 37-58.
13. B. Valeur and M. N. Berberan-Santos, Molecular Fluorescence. Principles and Applications, Wiley VCH, New York, Second edn., 2012.
14. M. Shinitzky and Y. Barenholz, Biochimica Et Biophysica Acta, 1978, 515, 367-394.
15. F. Jahnig, P Natl Acad Sci USA, 1979, 76, 6361-6365.
16. K. Fushimi and A. S. Verkman, J Cell Biol, 1991, 112, 719-725.
17. K. Luby-Phelps, S. Mujumdar, R. B. Mujumdar, L. A. Ernst, W. Galbraith and A. S. Waggoner, Biophys J, 1993, 65, 236-242.
18. M. A. Haidekker, T. T. Ling, M. Anglo, H. Y. Stevens, J. A. Frangos and E. A. Theodorakis, Chem Biol, 2001, 8, 123-131.
19. B. D. Allen, A. C. Benniston, A. Harriman, S. A. Rostron and C. Yu, Phys Chem Chem Phys, 2005, 7, 3035-3040.
20. M. A. H. Alamiry, A. C. Benniston, G. Copley, K. J. Elliott, A. Harriman, B. Stewart and Y. G. Zhi, Chem Mater, 2008, 20, 4024-4032.
21. M. K. Kuimova, G. Yahioglu, J. A. Levitt and K. Suhling, J Am Chem Soc, 2008, 130, 6672-6673.
22. Y. Wu, M. Stefl, A. Olzynska, M. Hof, G. Yahioglu, P. Yip, D. R. Casey, O. Ces, J. Humpolickova and M. K. Kuimova, Phys Chem Chem Phys, 2013, 15, 14986-14993.
23. R. Sachl, I. Boldyrev and L. B. Johansson, Phys Chem Chem Phys, 2010, 12, 6027-6034.
24. R. Sachl, E. Rosenbaum, M. Sellstedt, F. Almqvist and L. B. Johansson, Langmuir, 2011, 27, 1662-1667.
25. P. Jurkiewicz, A. Olzynska, M. Langner and M. Hof, Langmuir, 2006, 22, 8741-8749.
26. K. Takakura, T. Toyota and T. Sugawara, J Am Chem Soc, 2003, 125, 8134-8140.
27. D. J. S. Birch, G. Hungerford and R. E. Imhof, Review of Scientific Instruments, 1991, 62, 2405-2408.
28. M. T. Stockl and A. Herrmann, Biochim Biophys Acta, 2010, 1798, 1444-1456.
29. M. Stefl, N. G. James, J. A. Ross and D. M. Jameson, Anal Biochem, 2011, 410, 62-69.
30. J. Baumann and M. D. Fayer, J Chem Phys, 1986, 85, 4087-4107.
31. R. Koynova and M. Caffrey, Bba-Rev Biomembranes, 1998, 1376, 91-145.
32. T. Baumgart, G. Hunt, E. R. Farkas, W. W. Webb and G. W. Feigenson, Biochim Biophys Acta, 2007, 1768, 2182-2194.
33. J. J. Fisz, J Phys Chem A, 2007, 111, 8606-8621.
34. S. Brasselet, P. Ferrand, A. Kress, X. Wang, H. Ranchon and A. Gasecka, in Fluorescent Methods to Study Biological Membranes, eds. Y. Mely and G. Duportail, Springer Verlag, Heidelberg, 2013, vol. 13.
35. S. Timr, A. Bondar, L. Cwiklik, M. Stefl, M. Hof, M. Vazdar, J. Lazar and P. Jungwirth, J Phys Chem B, 2014, 118, 855-863.
36. L. M. Loew, G. W. Bonneville and J. Surow, Biochemistry, 1978, 17, 4065-4071.

37. T. Baumgart, A. T. Hammond, P. Sengupta, S. T. Hess, D. A. Holowka, B. A. Baird and W. W. Webb, Proc Natl Acad Sci U S A, 2007, 104, 3165-3170.
38. I. Levental, M. Grzybek and K. Simons, Proc Natl Acad Sci U S A, 2011, 108, 11411-11416.
39. P. G. Saffman and M. Delbruck, Proc Natl Acad Sci U S A, 1975, 72, 3111-3113.
40. B. D. Hughes, B. A. Pailthorpe and L. R. White, J Fluid Mech, 1981, 110, 349-372.
41. K. Weiss, A. Neef, Q. Van, S. Kramer, I. Gregor and J. Enderlein, Biophysical Journal, 2013, 105, 455-462.
42. E. P. Petrov and P. Schwille, Biophys J, 2008, 94, L41-43.

FIGURE LEGENDS

Figure 1. Structures of compounds used in this study.

Figure 2. a) Excitation and emission spectra of the studied rotational BODIPY probes in methanol/chloroform (1:1, v:v) solution at room temperature. Identities of the excitation and emission curves are given in Table 1. b) Fluorescence lifetime of the studied rotational BODIPY probes embedded in DMPC large unilamellar vesicles as a function of temperature.

Figure 3. An illustration of FRET experiment in a lipid bilayer containing donor (compounds **1**, **2b** or **3b**; green ellipsoids) and acceptor (DiD; blue ellipsoids) molecules. The yellow arrows indicate possible energy transfer events from the donors to the acceptors. The plane to plane distance d_A corresponds to FRET from the donors to the acceptors localised in the same leaflet whereas the distance d_B corresponds to FRET from the donors to the acceptors residing in the opposite leaflet.

Figure 4. Fluorescence lifetime decays of compounds **1**, **2b** and **3b** measured in GUVs composed of DOPC (Ld phase), DPPC:cholesterol (2.2:1; Lo phase), and DPPC (So phase) at room temperature.

Figure 5. Fluorescence anisotropy confocal imaging of **1** (a, b, c, d), **2b** (e, f, g, h), and **3b** (i, j, k, l) BODIPY-based molecular rotors embedded in GUVs composed of either DOPC (a, e, i; Ld phase) or DPPC (b, f, j; So phase) measured at room temperature. Excitation light was polarized along the Y axis (see the green arrow in panel a). Presented pseudo-colour anisotropy images are examples of GUV cross sections in the X-Y middle plane. Anisotropy as a functions of the ρ contour angle around the GUV cross section (c, g, k) were averaged over at least 3 different GUVs (ρ angle is defined in panel a). A schematic orientation of the electronic transition dipole moment of the fluorophores in the liposomal membrane that agrees with the obtained results is depicted in panels d, h, l in the form of black and blue arrows.

Table 1 Fluorescence properties of the studied compounds measured in solution (chloroform:methanol) and in DMPC, POPC and DPPC lipid vesicles.

Dye	chloroform:methanol			DMPC				POPC	DPPC
	EX / EM[a]	ε[b]	Φ[c]	$\Delta\lambda$[d] 10→40°C	$\Delta\tau$[e] 25→20°C	$\tau_{20°C}$ / $\tau_{25°C}$[f]	$\Delta\tau/\Delta T$[g] 25→40°C	K_D[h] (acrylamide)	F_0/F[i] (16-Doxyl)
	nm	$M^{-1}\cdot cm^{-1}$		nm	ns		$ns\cdot K^{-1}$	M^{-1}	
1	496 / 513	60 000	0.15	0.2	0.35	1.20	0.04	0.060 ± 0.020	1.7 ± 0.1
2a	501 / 518	11 000	0.02	3.0	1	1.40	0.06	n.d.	n.d.
2b	511 / 525	39 000	0.11	1.6	0.65	1.10	0.07	0.020 ± 0.010	3.8 ± 0.1
3a	500 / 517	39 000	0.006	–[j]	0.70	1.55	0.03	n.d.	n.d.
3b	511 / 528	140 000	0.04	2.7	0.45	1.10	0.03	0.035 ± 0.020	4.5 ± 0.1

[a] maxima of the fluorescence excitation and emission spectra, [b] extinction coefficient, [c] fluorescence quantum yield ([a-c] chloroform:methanol, 1:1, v:v), [d] shift of the mean emitted wavelength upon heating from 10 to 40°C, [e] fluorescence lifetime change upon the main phase transition, $\Delta\tau_{25->20°C} = \tau_{20°C} - \tau_{25°C}$, [f] mean fluorescence lifetimes ratio at the main phase transition, [g] fluorescence lifetime change per degree of K in the Ld phase, [h] Stern-Volmer quenching constant for the water-soluble acrylamide quencher ([d-h] POPC LUVs), [i] quenching ratio for 16-Doxyl quencher embedded in DPPC MLVs at 60°C (F_0 and F are fluorescence intensities in the absence and presence of the quencher, respectively), [j] the change cannot be quantified due to very low fluorescence signal. n.d. – not determined.

Table 2. Mean fluorescence lifetimes of molecular probes in different lipid phases. Lifetimes were obtained by mono/bi-exponential tail-fitting of decays measured in GUVs by FLIM method. The last column contains information on the Förster radius of the compounds with DiD dye.

Probe	τ_{Ld}/ ns	τ_{Lo}/ ns	τ_{So}/ ns	R_0/Å
1	1.8 ± 0.1	2.9 ± 0.1	4.5 ± 0.2	49
2b	5.7 ± 0.1	5.7 ± 0.1	7.0 ± 0.2	49
3b	5.1 ± 0.1	5.4 ± 0.2	6.9 ± 0.1	42

Graphical Abstract for TOC

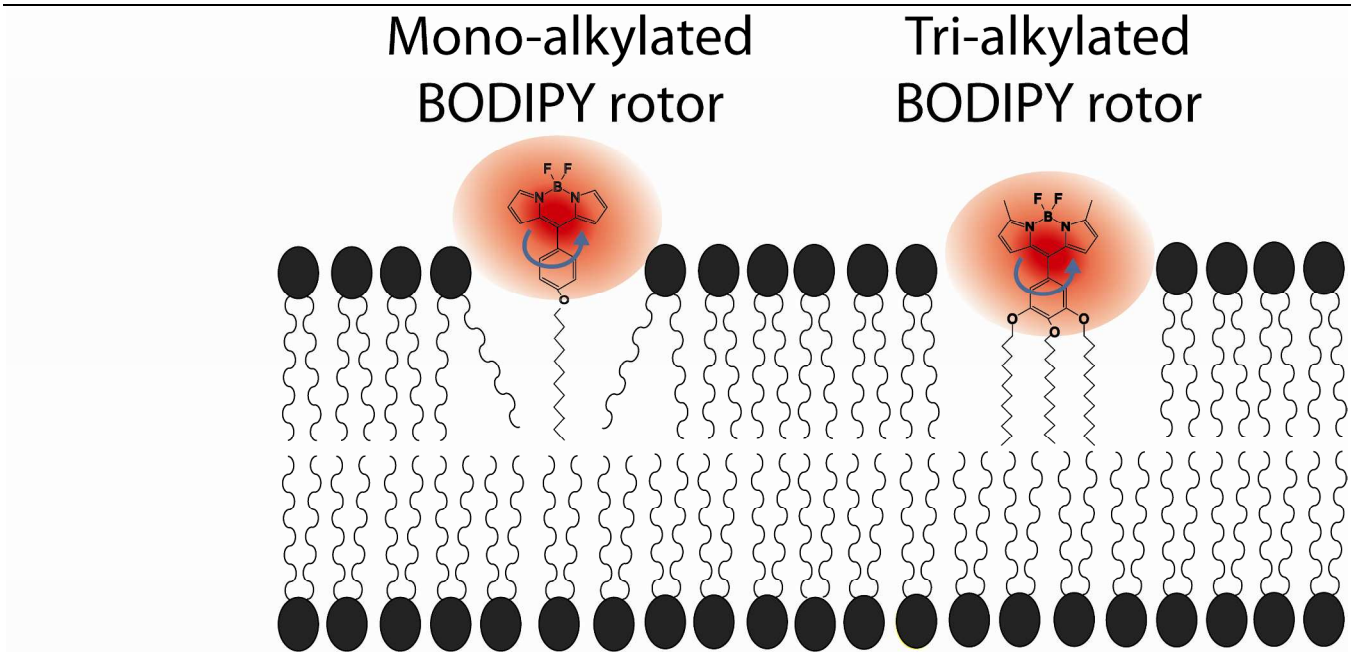

Di- and tri-alkylated variant of BODIPY rotor: carefully characterised probes sensing liquid or gel state of lipid membranes.